

Incorporating different tidal energy device designs into 4D collision risk simulations allowing increased flexibility for industry

Nicholas Horne, Ross Culloch, Pal Schmitt and Louise Kregting

Abstract— The marine renewable energy industry has created a wide variety of device designs including horizontal and vertical axis tidal turbines. One key issue in consenting the devices is the risk of animal collision with the infrastructure. Current efforts in addressing collision risk use simplified analytical solutions to calculate probabilities over the swept area of a horizontal axis tidal turbine. However, this method is not appropriate for every device as there are a multiple different tidal energy device designs being tested including tidal kites and cross-flow turbines. The 4D collision risk model is a simulation-based platform which, to date, has investigated a novel tidal energy kite, with a figure-of-eight trajectory, and its collision risk with an object. This earlier work demonstrated the effectiveness of this model to assess differences in collision risk due to variations in the device configuration. In a step change of this work we simulate the collision risk probabilities of three tidal devices: a horizontal axis turbine, a cross-flow turbine and a tidal kite. Here we demonstrate the flexibility and ease in which this 4D model can be adapted to any device type giving the user the ability to quantify a wide range of scenarios which could therefore be of use to developers, consultants and regulators for project design, assessments and licencing.

Keywords—Environmental Impact Assessment, Marine Mammals, Computer-aided design

I. INTRODUCTION

TIDAL energy has the potential to be a key contributor to global renewable energy targets in tackling climate change, as the predictability of the tidal cycle makes this an attractive option for many countries looking to expand their renewable energy sources [1]. Growth in the industry has led to the development of multiple tidal device designs, however there is still a lack of understanding on how marine fauna interact with these

devices. A key issue raised in the consenting process of tidal energy devices (TEDs) is the risk of animal collision. However, based on a growing body of research involving near-field monitoring and mitigation, with the primary focus being on protected species such as marine mammals [2],[3], there is no evidence of a collision having occurred, to-date.

Collision risk with renewable energy devices has been an ongoing concern since the 1980s, where studies investigating the occurrence of bird strikes with onshore wind energy devices counted the number of carcasses around wind turbines [4]. Byrne [4] only monitored this for five days, but in order to understand collision risk over the life of a turbine, a theoretical modelling approach was required, and so the Band model was developed [5]. The Band model [5], uses a formulaic approach to calculate a collision rate over a period of time (Eq.1).

$$CRM = D \times B \times CR \times v \times p_{coll} \quad (1)$$

Collision risk over a period of time (CRM) is calculated using the mean risk of a collision during a single transit (p_{coll}), animal speed (v), the number of rotors (B), cross-sectional (CR) and animal density (D). A collision is simply classified as an animal coming into contact with a device and does not necessarily equal a fatality. In the Band model the mean risk of a collision during a single transit, p_{coll} (Eq.1) is calculated using the device's blade characteristics and a simplified animal shape. Calculating the blade profile of a horizontal axis turbine is possible with this equation but with a device such as the Minesto DeepGreen kite the blade profile of the device is not suitable to be used in the calculation. Since its

ID:1641 Environmental impact and appraisal

This work is funded under The Bryden Centre for Advanced Marine & Bio-Energy Research, a project supported by the European Union's INTERREG VA Programme, managed by the Special EU Programmes Body (SEUPB) was based at Queen's University Belfast with affiliation to Scottish Association of Marine Science, University of Highland and Islands and Marine Scotland Science.

N. Horne is with the Marine Research Group, Queen's Marine Laboratory, 12-13 The Strand, Portaferry, Newtownards, Down, Northern Ireland, BT22 1QZ. (e-mail: n.horne01@qub.ac.uk).

R. Culloch is with Marine Scotland Science, 375 Victoria Rd, Aberdeen AB11 9DB (e-mail: ross.culloch@scotgov.com).

P. Schmitt is with the Marine Research Group, Queen's Marine Laboratory, 12-13 The Strand, Portaferry, Newtownards, Down, Northern Ireland, BT22 1QZ. (e-mail: p.schmitt@qub.ac.uk).

L. Kregting is with the Marine Research Group, Queen's Marine Laboratory, 12-13 The Strand, Portaferry, Newtownards, Down, Northern Ireland, BT22 1QZ. (e-mail: l.kregting@qub.ac.uk).

development the Band model has been adapted to assessing collision risk around horizontal axis TEDs [6].

In 2007 the Encounter Rate Model (ERM) was developed by Wilson *et al* [7] which also uses a formulaic approach to calculate the risk of collision between TEDs and animals. The difference between the two models is that the Band model calculates risk from the number of animal transits through the rotor whereas the ERM focuses on volume per unit time swept by each blade [6]. Despite their differences they both use a physical model of the rotor, the animal body size and swimming activity to calculate the probability of collision.

These models are well suited for horizontal axis turbines, which are the design-type in which the majority of modelling investigations have been carried out on (e.g. [7], [8] and [9]); which is unsurprising, as they are both similar designs to wind turbines and the first grid connected full scale tidal turbine, SeaGen (Fig. 1).



Fig. 1. SeaGen Tidal Turbine installed in Strangford Lough, Northern Ireland. The first commercial scale grid connected tidal turbine in the world.

Since the installation of SeaGen in 2008, further development of horizontal axis turbines such as the Atlantis AR1500 (Fig. 2.) have led to increased complexity in design. Modelling efforts assume a single blade profile with a mean speed of rotation for assessing collision risk, however many horizontal axis turbines can change the pitch of the blades and rotate the rotor to face the incoming tide [10]. Not all devices are horizontal axis turbines, designs such as the tidal kite, Archimedes screws, vertical axis and paddle devices have been proposed [11]. In North America, the ORPC TidGen device (a cross-flow turbine using a Gorlov helical design to harness tidal power) is being tested and installed, and in the United Kingdom the Minesto DeepGreen tidal kite is being tested. These two device designs have a complexity of design that cannot be captured in collision risk models, to-date.

In 2017, Schmitt *et al* [12] presented a simulation-based approach to collision risk modelling to offer a solution for assessing unique tidal energy devices. The 4D model (3D space over time) assessed collision probabilities between the quarter-scale Minesto DeepGreen kite and an object (based loosely on an adult harbour seal), using a uniform distribution of objects passing throughout the swept area

of the device. This work also investigated how altering parameters that influenced the device flight path affected collision probabilities. The model was developed within the software, freeCAD [13] which is an open-source computer aided design software that can be run using the coding language, python.



Fig. 2. Model representation of Atlantis AR1500 horizontal axis tidal turbine installed in the Pentland Firth, Scotland.

The work presented herein further develops the 4D model using the software package Blender [14], which is an open-source game design software. Blender is a similar computer aided design software that uses the coding language python, but with additional flexibility allowed by the game-engine for detailed inputs (e.g. angle of approach) and fast, accurate real time physical space for simulations. To demonstrate that multiple different TEDs can be simulated using the 4D model approach, this paper builds on Schmitt *et al* [12], and presents three hypothetical case studies using different TEDs: a tidal kite, a cross-flow turbine and a horizontal axis turbine.

II. METHODS

A. Model Development

Within Blender, three 3D shapefiles were created to represent the devices being simulated in this paper: a tidal kite (Fig. 5), a cross-flow turbine (Fig. 6) and a horizontal axis turbine (Fig. 7). The devices were created with both static parts (e.g. foundation) and moving parts (e.g. rotor) and were modelled in two files (static and moving). The moving parts then required the motion to be configured to match the movement of the device. This was done using the game-engines motion input which can give an object different motion, such as linear and rotational velocity.

For a single simulation the starting position of the device's moving parts will affect the chances of a collision occurring. Therefore, in order to get a probability of a collision, multiple simulations must be run over the time it takes for one full transit of a device's moving part(s), for example, one full rotation of a turbine rotor. Each

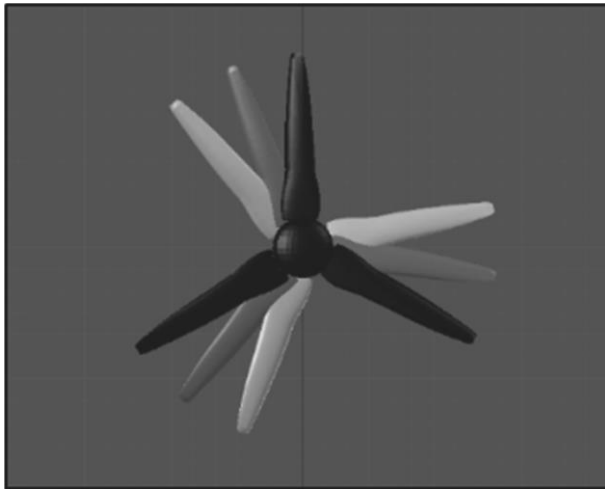


Fig. 3. Example of a turbine rotor starting positions with time lag of 0 (black), 1 (dark grey) and 2 (light grey).

simulation must have a different starting position of the device's moving part(s), which is input to a simulation via a time lag; an example of three different time lags can be seen in Fig. 3. Each device requires time lags to be set according to the time taken for the completion of one full transit of the device's moving parts.

B. Tidal Kite

The 3D shapefile for the tidal kite used in Schmitt et al [12] was adapted for use in Blender. The simulation was run for a quarter scale model with a 12m wingspan based on the 3kW Minesto DeepGreen Kite (Fig. 4.) currently being tested in Strangford Lough, UK. The figure of eight flight path requires a set of three equations to produce a rotation vector for each timestep of a simulation. A detailed description of these equations can be found in Schmitt et al [12]. The flight path for these simulations are presented in Table I. and the 3D shapefile used, is shown in Fig. 5.

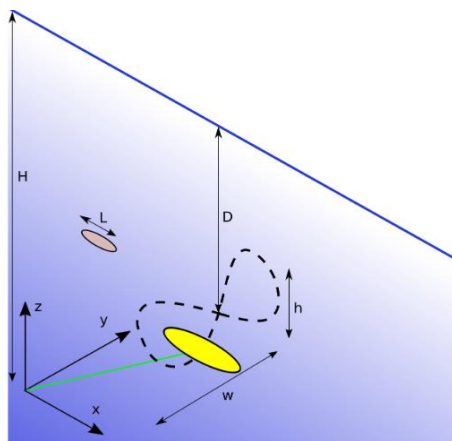


Fig. 4. Schematic illustration of the tidal kite (yellow), tether (green) and flight path (dashed line) with main variables as defined in Table 1 and coordinate system as used in the simulations. The grey elliptic symbol represents the animal under risk of collision. The foundation is located at the origin.

The tether and kite are defined as two separate shapefiles in order to differentiate collisions between them.

TABLE I
FLIGHT PATH PARAMETERS FOR TIDAL KITE SIMULATIONS
WITH THE RELEVANT PARAMETERS IDENTIFIED IN FIG. 4. IN
PARENTHESES.

Parameter	Input
Water Depth (D)	30m
Figure width (w)	10m
Figure height (h)	3m
Figure period	8s
Tether Length	20m
Kite wingspan	3m

Starting positions for an area of 14m wide and 20m high were used with 50 time lags over 8 seconds (the time taken for a full rotation) as per Schmitt et al [12], creating 15,750 simulations.

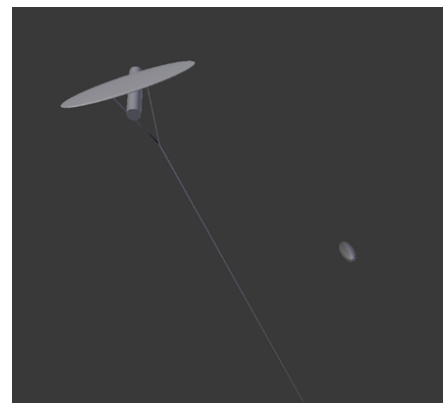


Fig. 5. Screenshot from Blender of the tidal kite 3D shapefile and the ellipsoid object of the seal in the simulations presented

C. Cross-flow turbine

The cross-flow turbine was adapted from a free Gorlov helical design wind energy device 3D shapefile [15] and the device base and overall design was built to represent a device similar to the 150kW ORPC TidGen® device. The structure was based upon Fig. 6. from Viehman [16] with the static parts (base) of the device as a separate shapefile from the moving parts (rotor), parameters used can be seen in Table II..

TABLE II
PARAMETERS USED FOR DESIGN AND SIMULATION OF CROSS-FLOW
TURBINE.

Parameter	Input
Number of rotors	4
Rotor diameter	2.8m
Rotor Width	4m
Power output	150kW
Tip speed ratio	2

The rotational speed for the rotor part of this device was run using a tidal speed of 3ms^{-1} and with a tip-speed ratio of 2 [17]. This meant that the rotational speed of the device was 2.129 radians per second.

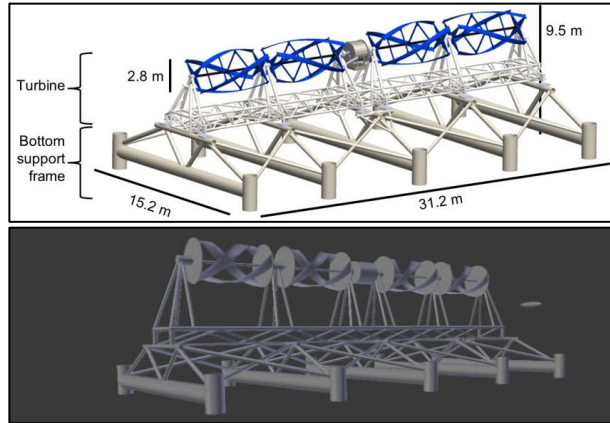


Fig. 6. Ocean Renewable Power Company's TidGen® Power System. Turbine image provided by ORPC (Top), Device structure was taken from the diagram in Viehman [16] and a screenshot from Blender of the 3D shapefile created from the design with the ellipsoid object of the seal for scale purposes (Bottom).

Starting positions were run for a 35m wide and 11m high area and with 50 time lags over the 2.9321 seconds taken for one full rotation of the rotor, creating 19,250 simulations. Lags were not tested further, as 50 time lags is accurate enough over the longer time period of the tidal kite [12].

D. Horizontal axis turbine

The horizontal axis turbine used was adapted from a free 3D shapefile [18] and adapted to have characteristics similar to the 1500kW Atlantis AR1500 device [19]. The device characteristics are displayed in Table. III.

TABLE III
INPUT PARAMETERS FOR THE DESIGN AND SIMULATION OF A
HORIZONTAL AXIS TURBINE, BASED ON AVAILABLE INFORMATION ON
THE AR1500 [19].

Parameter	Input
Number of blades	3
Rotor diameter	18m
Hub size	2.4m
Turbine length	12m
Power output	1500kW
RPM	14

The Atlantis AR1500 is described as rotating at 14RPM equating to 1.466 radians per second, which was used as the rotational speed for these simulations. The starting positions of the animal were simulated over an area of 35m wide and 20m high. 50 time lags over the 4.29s period for a full rotation were used for each starting position, creating 48,050 simulations. Lags were not tested further as 50 lags was accurate enough over the longer time period of the tidal kite [12].



Fig. 7. Screenshot of 3D shapefile of the horizontal axis turbine design, the ellipsoid object of the seal can be seen for scale purposes.

E. Simulations

The animal shape is created from an ellipsoid representing the dimensions of an adult harbour seal, length of 1.41m and width 0.3m, based on recommendations from Scottish Natural Heritage [6]. This was used for all devices and the swim speed of the seal object was 1.8ms^{-1} for all simulations.

The simulations in this paper are run with a 1m by 1m grid of fixed starting positions, set to be wider than the width and height of the area the device occupies during operation. For each starting position a set of time lags are set in order to obtain a probability of collision for each point on the device. These steps create the configuration for a set of simulations for a single device (Fig. 8.).

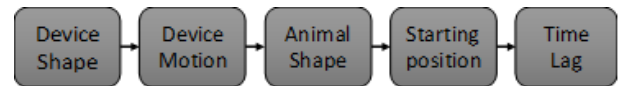


Fig. 8. Schematic of model configuration required to run a set of simulations.

F. Analysis

The probability of a collision occurring from each starting position was calculated from the number of collisions at a starting position divided by the number of lags (i.e. 50 in this case). This was then used to display the collision percentage at each position, and the output was displayed using ggplot2 [20] in R [21].

The collision probability used in the Band model (p_{coll} ; Eq.1) refers only to the swept area of the turbine and therefore, to be consistent with this approach, herein, only the moving parts of the devices were used to calculate the chance of collision. In order to calculate the percentage chance of a collision in the swept area of each simulated device, the following calculation is used on the output data:

$$PS_{\text{sweptA}} = N_{\text{Coll}} / \left(\frac{N_{\text{CollPos}}}{N_{\text{lags}}} \right) \times 100 \quad (2)$$

Where $NColl$ is the number of collisions and $NCollPos$ is the number of positions at which at least one collision occurred for all time lags tested. $Nlags$ is the number of time lags for each starting position. All post processing of the data generated was implemented in R.

III. RESULTS

G. Tidal Kite

Fig. 9 & 10. present the distribution of collisions from the tidal kite simulations, displaying the collisions of the seals with the kite (Fig. 9.) and the entire structure (Fig. 10.), both through the shading and size of the points, where darker and larger points indicate a higher chance of collision. Fig. 9. shows the figure of eight movement, passing through the centre twice in a single rotation, resulting in a higher percentage of collisions as compared to the outer edges of the flight path.

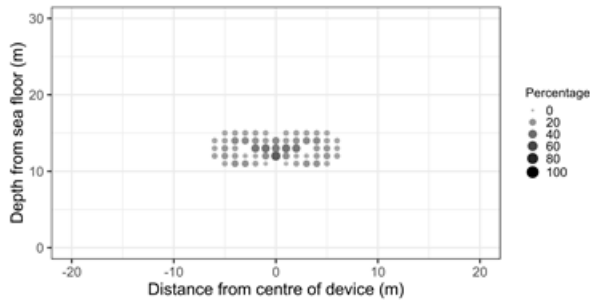


Fig. 9. Percentage chance (%) of a collision at each starting position between an animal and the kite only. Darker shades and larger dots indicate a higher chance of collision (Number of simulations = 15,750).

Fig. 10. shows collision percentages for both the tether and the kite, note that at the base of the tether, the area of the device with little to no movement, there is a 100% chance of collision. The tidal kite had a $PSweptA$ of 20.6%, which was calculated using the collisions with both the kite and tether, as both are moving.

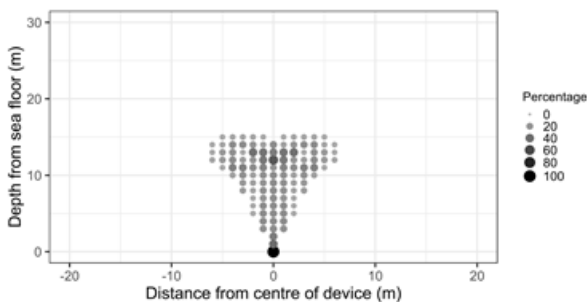


Fig. 10. Percentage chance (%) of a collision at each starting position between an animal and the whole tidal kite device. Darker shades and larger dots indicate a higher chance of collision (Number of simulations = 15,750).

H. Cross-flow Turbine

Fig. 11 & 12. present the distribution of collisions from the cross-flow device simulations. It displays the collisions with the rotor and the entire structure, both through the shading and size of the points. Fig. 11. shows the collision

percentages over the swept area of the device, i.e. the moving parts of the device.

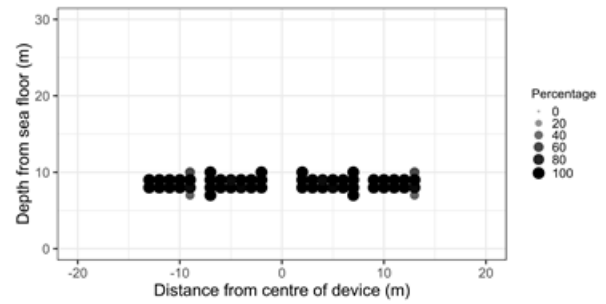


Fig. 11. Percentage chance (%) of a collision at each starting position between an animal and rotor only. Darker shades and larger dots indicate a higher chance of collision (Number of simulations = 19,250).

Fig. 12. shows the collision percentages for the whole device (i.e. moving and static parts, the latter of which has a 100% chance of collision). A $PSweptA$ of 96.0% for the cross-flow device was calculated for the rotor (i.e. excluding the static part of the device). This was done as the rotor is the moving only part of the device, and is therefore the only component contributing to the swept area.

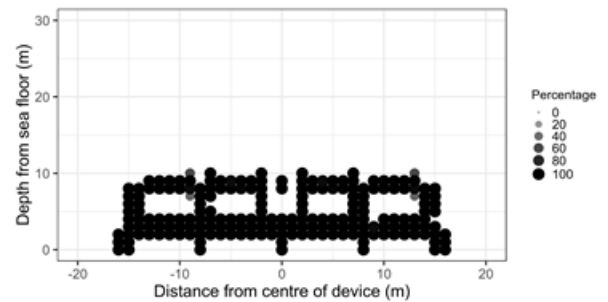


Fig. 12. Percentage chance (%) of a collision at each starting position between an animal and whole cross-flow device. Darker shades and larger dots indicate a higher chance of collision (Number of simulations = 19,250).

I. Horizontal Axis Turbine

Fig. 13 & 14. present the distribution of collisions from the horizontal axis device simulations. It displays the collisions with the rotor and the entire structure both through the shading and size of the points. Fig. 13. shows the collision percentages over the swept area of the device (i.e. for the parts of the device that are moving). Whereas Fig. 14. shows collision percentages for the entire device (i.e. the moving and static parts of the device, the latter of which has a 100% chance of collision). A $PSweptA$ of 81.4% for the cross-flow device was calculated for the rotor (i.e. excluding the static part of the device). This was done as the rotor is the only moving part, and is therefore the only component contributing to the swept.

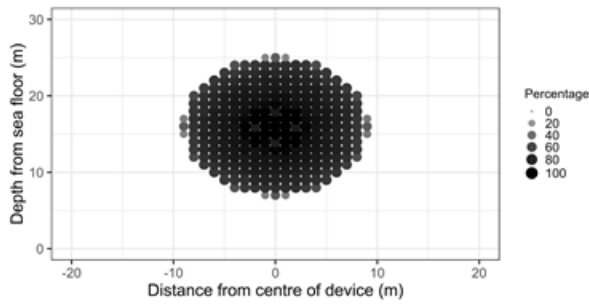


Fig. 13. Percentage chance (%) of a collision at each starting position between an animal and the rotor. Darker shades and larger dots indicate a higher chance of collision (Number of simulations = 48,050).

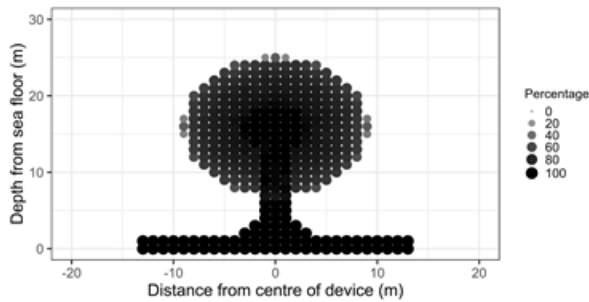


Fig. 14. Percentage chance (%) of a collision at each starting position between an animal and whole horizontal axis turbine. Darker shades and larger dots indicate a higher chance of collision (Number of simulations = 48,050).

IV. DISCUSSION

We have demonstrated the application of a 4D simulation-based approach to collision risk modelling that can tackle the issue of different TED designs. Using these basic scenarios to demonstrate the application of this approach does make comparisons somewhat irrelevant without consideration to area occupied and the potential influence of environmental and ecological factors, for example. It should also be noted that, as can be seen in Eq.1 the cross-sectional area of the device must be taken into account to understand overall collision risk. For example, the tidal kite has a flightpath that is a figure of eight 10m wide and 3m in height and therefore the cross-sectional area would give a larger collision risk when implemented to Eq.1.

The calculated PS_{sweptA} for each device are directly comparable to p_{coll} (Eq.1), with the additional benefit being that the simulation-based approach is capable of quantifying collision risk for novel device designs, such as those that cannot be calculated using the currently applied modelling methods. The simulations presented in this paper are based on a uniform distribution and do not incorporate ecological (with the exception of the size and shape of the object being based on an adult harbour seal) or environmental data, both of which are well documented as being important for better informing collision risk models [7]. These parameters could be integrated into this simulation-based approach, either as part of the

simulation or during post-processing. For example, using empirical studies on the likelihood of fatality through collision risk [22] as collisions on different points of the device may be less severe than others (e.g. the hub of the HAT vs the rotor tips), Blender offers a flexible and powerful system in which information such as speed of a collision could be extracted; this, could then be used to take a step further, with respect to estimating the proportion of collisions that are fatal.

Being an emerging industry, TEDs are continuously changing. Although most devices currently installed are horizontal axis turbines, other devices such as Minesto's sea kite are being installed in the UK and further afield (e.g. two 100kW devices have been sold for installation in the Faroe Islands [23]). Even as these devices are being installed improvements to the technology and design continue to progress at a rapid rate, for example, Minesto have announced a new improved wing design [24]. In the development stages 3D shapefiles are used in testing and advertising [25]. As these files already exist it is straightforward for developers to use these shapefiles, which can be quickly and easily implemented into this simulation-based modelling framework, as we have demonstrated here. This could potentially allow for more flexibility during the process of informing the EIA for turbine design/parameters, for example, variations in flightpath parameters of the tidal kite may reduce impact on a protected species.

This paper serves to illustrate the flexibility of this simulation-based approach, whilst providing an insight into the potential for incorporating parameters of interest into collision risk assessment (e.g. size and swim speed of animals), which would give different collision risk estimates. Furthermore, this approach could be used to assess sensitivities in parameters and the uncertainties, the outputs of which could then be used to provide recommendations on the areas in which targeted research is needed in order to reduce uncertainty around the most influential parameters in collision risk modelling.

ACKNOWLEDGEMENT

This work is funded under The Bryden Centre for Advanced Marine & Bio-Energy Research, a project supported by the European Union's INTERREG VA Programme, managed by the Special EU Programmes Body (SEUPB) was based at Queen's University Belfast with affiliation to Scottish Association of Marine Science, University of Highland and Islands and Marine Scotland Science.

REFERENCES

- [1] Z. Zhou, M. Benbouzid, J. F. Charpentier, F. Scuiller, and T. Tang, "Developments in large marine current turbine technologies—A review," *Renewable and Sustainable Energy Reviews*, vol. 71, pp. 852-858, 2017.
- [2] C. Sparling, M. Loneragan, and B. McConnell, "Harbour seals (*Phoca vitulina*) around an operational tidal turbine in Strangford Narrows: No barrier effect but small changes in

- transit behaviour," *Aquatic Conservation: Marine and Freshwater Ecosystems*, vol. 28 no. 1, pp. 194-204, 2018.
- [3] R. Joy, J. D. Wood, C. E. Sparling, D. J. Tollit, A. E. Copping, and B. J. McConnell, "Empirical measures of harbor seal behavior and avoidance of an operational tidal turbine," *Marine pollution bulletin*, vol. 136, pp. 92-106, 2018.
 - [4] S. Byrne. "Bird movement and collision mortality at a large horizontal axis wind-turbine," *Cal-Neva Wildlife Transactions*, pp. 76-83, 1983.
 - [5] W. Band. "Windfarms and Birds: calculating a theoretical collision risk assuming no avoiding action," Scottish Natural Heritage, Scotland, 2000. [Online] Available: <http://www.snh.gov.uk/planning-and-development/renewable-energy/onshore-wind/assessing-bird-collision-risks/>
 - [6] Scottish Natural Heritage. "Assessing collision risk between underwater turbines and marine wildlife", Scottish Natural Heritage, Scotland. [Online] Available: <https://www.nature.scot/sites/default/files/2017-09/Guidance%20Note%20-%20Assessing%20collision%20risk%20between%20underwater%20turbines%20and%20marine%20wildlife.pdf>
 - [7] B. Wilson, R. S. Batty, F. Daunt, and C. Carter, "Collision risks between marine renewable energy devices and mammals, fish and diving birds," Scottish Association for Marine Science, Oban, Scotland. 2007. [Online] Available: <https://tethys.pnnl.gov/sites/default/files/publications/Wilson%20et%20al%202007.pdf>
 - [8] L. Hammar, L. Eggertsen, S. Andersson, J. Ehnberg, R. Arvidsson, M. Gullstöm, and S. Molander, "A probabilistic model for hydrokinetic turbine collision risks: exploring impacts on fish," *PloS one*, vol. 10, no. 3, 2015. DOI: <https://doi.org/10.1371/journal.pone.0117756>, [Online].
 - [9] A. Copping, M. Grear, R. Jepsen, C. Chartrand, and A. Gorton, "Understanding the potential risk to marine mammals from collision with tidal turbines," *Int. Journ. Mar. Energy*, vol. 19, pp. 110-123, 2017.
 - [10] Atlantis Resources, Simec Atlantis, (2019, Feb, 11), MeyGen Update [Blog]. Available: <https://simecatlantis.com/2019/02/11/meygen-update-3/>
 - [11] European Marine Energy Centre, (2019), Tidal Devices. [Online]. Available: <http://www.emec.org.uk/marine-energy/tidal-devices/>
 - [12] P. Schmitt, R. Culloch, L. Lieber, S. Molander, L. Hammar, L. Kregting, "A tool for simulating collision probabilities of animals with marine renewable energy devices," *PloS one*, vol. 12, no.11, 2017. DOI: <https://doi.org/10.1371/journal.pone.0188780>
 - [13] The FreeCAD Team, FreeCAD. [Software]. Available: <https://www.freecadweb.org/>
 - [14] Blender Foundation, Blender. [Software]. Available: <https://www.blender.org>
 - [15] The-brandals, GORLOV Wind Turbine Free 3D model, Dec, 2014. [Online]. Available: <https://www.cgtrader.com/free-3d-models/architectural/engineering/gorlov-wind-turbine>
 - [16] Viehman, H. (December, 2016). Hydroacoustic Analysis of the Effects of a Tidal Power Turbine on Fishes. (Doctoral thesis). Retrieved from https://www.researchgate.net/publication/312374274_Hydroacoustic_Analysis_of_the_Effects_of_a_Tidal_Power_Turbine_on_Fishes.
 - [17] P. Bachant, and M. Wosnik, "Characterising the near-wake of a cross-flow turbine," *Journal of Turbulence*, vol. 16, no. 4, pp. 392-410, 2015.
 - [18] 375designs, Tidal Stream Turbine. [Online].(2014). Available: <https://www.cgtrader.com/free-3d-models/industrial/machine/tidal-stream-turbine>
 - [19] Atlantis Resources. (2016). AR1500 Tidal Turbine Brochure, Simec Atlanstis. Retrieved from <https://simecatlantis.com/wp-content/uploads/2016/08/AR1500-Brochure-Final-1.pdf>.
 - [20] H. Wickham, ggplot2: Elegant Graphics for Data Analysis, Springer-Verlag [Online]. 2016.
 - [21] R Core Team, R: A language and environment for statistical computing, R Foundation for Statistical Computing. [Online] Available: <https://www.R-project.org/>
 - [22] D. Thompson, A. Brownlow, J. Onoufriou, and S. E. W. Moss, "Collision risk and impact study: Field tests of turbine blade-seal carcass collisions," Sea Mammal Research Unit, St Andrews, Scotland. 2015. [Online]. Available: http://www.smru.st-andrews.ac.uk/files/2015/10/MR7-2-3_collision_risk_impact_field_VF1.pdf
 - [23] Minesto, Faroe Islands – tidal to go 100% renewable by 2030. [Online]. Available: <https://minesto.com/projects/faroe-islands>
 - [24] Minesto, Minesto makes product development progress; sets DG100 wing specs, Feb, 2019. [Online]. Available: <https://minesto.com/news-media/minesto-makes-product-development-progress-sets-dg100-wing-specs>
 - [25] Offshore Renewable Energy Catapult (2016, Sept, 12), Atlantis Resources' AR1500 at ORE Catapult Blyth [Video file]. Retrieved from: <https://www.youtube.com/watch?v=9P57uLHqCyA>